




Endometrial Cancer Spheres Show Cancer Stem Cells Phenotype and Preference for Oxidative Metabolism

Maria João Carvalho^{1,2,3,4,5}  · Mafalda Laranjo^{2,3,4} · Ana Margarida Abrantes^{2,3,4} · João Casalta-Lopes^{2,3,4,6} · Daniela Sarmiento-Santos² · Tânia Costa² · Beatriz Serambeque² · Nuno Almeida² · Telmo Gonçalves² · Catarina Mamede^{2,3} · João Encarnação^{2,3} · Rui Oliveira⁷ · Artur Paiva⁸ · Rui de Carvalho⁹ · Filomena Botelho^{2,3,4} · Carlos Oliveira³

Received: 2 September 2018 / Accepted: 31 October 2018
© Arányi Lajos Foundation 2018

Abstract

This study aimed to characterize endometrial cancer regarding cancer stem cells (CSC) markers, regulatory and differentiation pathways, tumorigenicity and glucose metabolism. Endometrial cancer cell line ECC1 was submitted to sphere forming protocols. The first spheres generation (ES1) was cultured in adherent conditions (G1). This procedure was repeated and was obtained generations of spheres (ES1, ES2 and ES3) and spheres-derived cells in adherent conditions (G1, G2 and G3). Populations were characterized regarding CD133, CD24, CD44, aldehyde dehydrogenase (ALDH), hormonal receptors, HER2, P53 and β -catenin, fluorine-18 fluorodeoxyglucose (^{18}F]FDG) uptake and metabolism by NMR spectroscopy. An heterotopic model evaluated differential tumor growth. The spheres self-renewal was higher in ES3. The putative CSC markers CD133, CD44 and ALDH expression were higher in spheres. The expression of estrogen receptor (ER) α and P53 decreased in spheres, ER β and progesterone receptor had no significant changes and β -catenin showed a tendency to increase. There was a higher ^{18}F -FDG uptake in spheres, which also showed a lower lactate production and an oxidative cytosol status. The tumorigenesis in vivo showed an earlier growth of tumours derived from ES3. Endometrial spheres presented self-renewal and differentiation capacity, expressed CSC markers and an undifferentiated phenotype, showing preference for oxidative metabolism.

Keywords Endometrial neoplasms · Neoplastic stem cells · Glucose metabolism

Introduction

Cancer stem cells (CSC) are a minor population of tumour cells which are capable of self-renewal, originating progenitor cells that differentiate aberrantly and do not respond adequately to homeostatic controls. This is in agreement with the theory of CSC which assumes the presence of a subpopulation

responsible for tumour maintenance, dissemination, and recurrence [1].

The endometrium has a unique regenerative capacity that is observed every menstrual cycle and in several periods of reproductive life. Endometrial stem cells have been identified considering clonogenic capacity, side population and label retaining cells [2–4]. The evidence of CSC in endometrial

✉ Maria João Carvalho
mariajoaosflcarvalho@gmail.com

¹ Gynecology Service, Coimbra Hospital and University Centre, Coimbra, Portugal
² Biophysics Institute, Faculty of Medicine, University of Coimbra, Coimbra, Portugal
³ Institute for Clinical and Biomedical Research (iCBR), area of Environment Genetics and Oncobiology (CIMAGO), Faculty of Medicine, University of Coimbra, Coimbra, Portugal
⁴ CNC.IBILI, University of Coimbra, Coimbra, Portugal

⁵ University Clinic of Gynecology, University of Coimbra, Coimbra, Portugal
⁶ Radiotherapy Service, Coimbra Hospital and University Centre, Coimbra, Portugal
⁷ Pathology Service, Coimbra Hospital and University Centre, Coimbra, Portugal
⁸ Flow Cytometry Unit, Coimbra Hospital and University Centre, Coimbra, Portugal
⁹ Centre for Functional Ecology, Department of Life Sciences, Faculty of Science and Technology, University of Coimbra, Coimbra, Portugal

cancer was associated with a functional profile and other characteristics such as CSC markers [5]. Endometrial CSC were described in primary endometrial carcinomas, identified by their clonogenic capacity and presence of genes associated with self-renewal [6]. The side population was also evaluated in endometrial cancer cell lines and primary tumours, representing 0.02–0.08% and 3.4% respectively. This minor population presented self-renewal, enhanced migration, lamellipodia and uropodia formation and tumorigenesis [7]. The side population was also associated with upregulation of genes related to epithelial to mesenchymal transition (EMT) [8].

CSC markers were already evaluated in endometrial tumours, namely markers related to embryonic development such as *MUSASHI-1*, *NANOG* and *OCT4*, and associated with this phenotype [6, 9, 10]. Regarding CD133, a positive population with self-renewal, it represented 5.7% to 27.4% in primary endometrial tumours and its expression was correlated with the worst prognosis [11, 12]. Likewise, the ALDH^{high} population was associated with a worse prognosis in endometrial cancer with differentiation markers, such as CD9, being absent in these cells [13].

Plasticity is another characteristic of CSC that is evident in resistance to treatment. The resistance mechanisms related to the endometrial CSC are influenced by the presence of ABC efflux transporters, ALDH activity, resistance to DNA damage, autophagy, resistance to apoptosis, activation of developmental pathways and microenvironment stimuli [5, 14]. Regarding endometrial CSC side population, CD133⁺ population showed decreased sensitivity to paclitaxel, doxorubicin and cisplatin [11, 13].

A comprehensive analysis of cell populations derived from an endometrial cancer cell line through a methodology involving a sphere forming protocol was performed, with respect to expression of CSC markers, hormonal receptors, EMT differentiation and metabolic profile. We also investigated the differential tumorigenicity in vivo of tumorspheres and derived adherent populations.

Materials and Methods

Cell Culture and Sphere-Forming Protocol

The human endometrioid carcinoma type I cell line (ECC-1) obtained from American Type Culture Collection (ATCC) in June 2012 was propagated in adherent conditions according to recommendations at 37 °C and 5% CO₂ in *Rooswell Park Memorial Institute 1640 Medium* (RPMI 1640, Sigma R-R6504) with 5% fetal bovine serum (Sigma F-7524), 400 µM sodium pyruvate (Gibco, 11360) and 1% antibiotic (100 U/mL of penicillin and 10 µg/mL streptomycin; Sigma A5955).

The sphere-forming protocol was adapted from previous descriptions [15–17]. The ECC-1 cell line was cultured during 5 days in *Dulbecco's Modified Eagle Medium* and the mixture of *Ham's F12* nutrients at a ratio of 1:1 (Sigma, DMEM-F12 D8900), supplemented with 100 µM putrescine (Sigma, P7505), 1% insulin-transferrin-selenium-A (Gibco, 51300–044) and 1% methylcellulose (Sigma, M7027) in suspension culture appropriate flasks (Sarstedt 83.1813.502) or plates (Costar, 3548), previously coated with poly(2-hydroxyethyl-methacrylate) (Sigma, P3932). Every two days, basic fibroblast growth factor (bFGF, Sigma, F0291) and epidermal growth factor (EGF, Sigma, E9644), both at a concentration of 10 ng/mL, were added. On the fifth day, the first generation spheres, named ES1, were obtained and cells were collected for experiments or placed into standard culture conditions as previously described for the ECC-1 cell line. A monolayer of cells, named G1 (first generation of adherent cells derived from the spheres), was obtained. After reaching cell confluence of 85–90% cells were detached and collected for experiments or for repetition of the sphere-forming protocol in order to obtain secondary sphere cultures, named ES2. This procedure was repeated successively in order to obtain three spheres (ES1, ES2 and ES3) and three adherent populations (G1, G2 and G3).

Sphere-Forming Capacity, Self-Renewal, Cloning Efficiency

In order to evaluate the capacity that each adherent cells possesses to originate spheres, ECC-1, G1 and G2 cells were cultured in sphere forming protocol conditions at a concentration of 8×10^4 cells/mL. After five days, the spheres with more than 40 µm in diameter were counted.

To evaluate self-renewal (ability of sphere cells to originate new colonies of spherical cells in suspension) cells isolated from ES1, ES2 and ES3 were cultured in sphere-forming protocol conditions at a concentration of 8×10^4 cells/mL. After eight days, the spheres with more than 40 µm in diameter were counted.

To access cloning efficiency (capacity of a cell to generate an adherent colony of 50 or more cells) ECC-1, ES1, ES2, ES3, G1, G2 and G3 were submitted to the clonogenic assay as described [18]. The number of colonies was recorded twelve days after plating.

Flow Cytometry

The expression of CD24, CD44 and CD133 in ECC-1, ES1, ES2, ES3, G1, G2 and G3 was assessed using flow cytometry. Suspensions of 10^6 cells in 100 µL of phosphate-buffered saline (PBS; in mM: 137 NaCl, 2.7 KCl, 10 Na₂HPO₄, and

1.8 KH₂PO₄ [pH 7.4]) were labelled with anti-CD24 (Beckman Coulter, PNIM2645), anti-CD44 (BioLegend, 103,020) and anti-CD133 (Miteny Biotec, 293C3-PCA) according to the manufacturer's recommendations. Subsequently, cell suspensions were evaluated in a FACS-Canto II flow cytometer (BD, San Jose, CAA) and analysed with FACSDiva software (BD, San Jose, CA).

Western Blot

The expression of ALDH, β -catenin, HER2, oestrogen receptor- α (ER α), oestrogen receptor- β (ER β), progesterone receptor (PR) and P53 was evaluated by western blot, as previously described [19]. Briefly, total protein extracts of ECC-1, ES1, ES2, ES3, G1, G2 and G3 were prepared. After SDS-PAGE proteins were electron-transferred to polyvinylidene fluoride membranes. Incubation with primary antibodies was performed overnight at 4 °C with constant stirring. For the detection of proteins of interest the following antibodies were used: anti-ALDH 1/2 H-8 (SC-166362, Santa Cruz Biotechnology, Inc.), anti- β -actin (Sigma-Aldrich, A5316), anti- β -catenin (Santa Cruz Biotechnology, Inc., sc7963), anti-p53 DO7 (Santa Cruz Biotechnology, Inc., sc-47,698), anti-ER α (Abcam, ab1104), anti-ER β X-24 (Santa Cruz Biotechnology, Inc., sc-133,554) and anti-SP2 PR (Abcam, ab27161). Incubation with the appropriate secondary antibody, namely anti-mouse (GE Healthcare, RPN5781) or anti-rabbit (Santa Cruz Biotechnology, Inc., sc-2007), was performed at room temperature for about 1 h. The blots were stained with fluorescent reagent elemental chlorine free (ECF Western Blotting Reagent Pack, Amersham Biosciences, UK) and developed in fluorescence scanner (Typhoon 9000 FLA, Sweden). In cases where the electrophoresis conditions do not provide retention of β -actin in the gel the membranes were first stained with Ponceau S (Sigma, P3504).

¹⁸F-FDG Uptake

¹⁸F-FDG uptake was evaluated in ECC1, ES1, ES2, ES3, G1, G2 and G3 as previously described [20]. Cell suspensions with 2×10^6 cells/mL were prepared and 925 Bq/mL of ¹⁸F-FDG was added to the cell culture medium. Five minutes after addition of the radiotracer and over 120 min with a 30-min interval, duplicate aliquots of 200 μ L of cell suspension were removed to eppendorf tubes containing cold PBS. The samples were then centrifuged at 5585 g for 60 s (Costar Spin Mini) to separate pellet and supernatant, the latter having being collected to another test tube. Radioactivity of both fractions (supernatant and pellet) was counted in a well scintillation counter (Capintec Inc., Model CRC - 15 W) in counts per minute (CPM) in order to determine the ¹⁸F-FDG uptake percentage by the cell populations.

NMR Spectroscopy

NMR isotopomer analysis of cell metabolism was performed as previously described [21, 22]. The ECC1 cell line, ES1 and G1 were cultured in the appropriate media but glucose was replaced by its uniformly enriched ¹³C isotopomer ([U-¹³C] glucose, Sigma, 389,374). After 24 h, the cultures were washed with PBS and lysed with ice cold methanol H₂O 80%:20% (v/v). The samples were centrifuged at 5725 g during 5 min in order to separate the aqueous phase from the pellet. After drying the aqueous phase, the resulting extracts were dissolved in a solution of sodium fumarate (10 mM) in D₂O (99.9%). Culture medium samples were analysed adding 40 μ L of the sodium fumarate D₂O solution.

The ¹H-NMR spectra were acquired in a 14.1 Tesla Varian NMR spectrometer using a 3 mm indirect detection probe, and consisted of 64 k points defining a spectral width of 7200 Hz. A total of 16 scans were acquired, using a 30° radiofrequency pulse and an interpulse delay of 10 s to ensure full relaxation. The ¹³C-NMR spectra were acquired in the same spectrometer but using a broadband 3 mm NMR probe, with waltz proton decoupling. Each spectrum consisted of 128 K points defining a spectral region of 35 kHz. To obtain a signal/noise ratio compatible with metabolic analysis between 15,000 and 20,000 transients were acquired, using a 45° radiofrequency pulse of and interpulse delay of 3 s, to ensure full relaxation of the aliphatic carbons. The analysis of the obtained ¹H- and ¹³C-NMR spectra was carried out using the software NUTSpro™ (Acorn NMR Inc., Livermore, CA).

Heterotopic Animal Model

The experimental protocol was approved by the Ethics Committee of the Medicine Faculty of Coimbra University (Ref: Of IBB/48/09). All experiments were performed in accordance with guidelines and regulations of the European Union. The Balb/c nu/nu mice were inoculated with ECC-1, ES1, ES2, ES3, G1, G2 and G3 (2×10^6 cells) into the dorsal region by subcutaneous injection and the heterotopic tumour growth was monitored weekly. Three animals per condition were inoculated. When the xenografts reached a volume of 100 mm³, growth was monitored daily for 10 days. The animals were euthanized and the tumours were excised for the histological study. The samples were fixed in buffered formalin at a concentration of 10%, dehydrated in increasing alcohol concentrations, cleared in xylene and embedded in paraffin. A random microtome was performed and the slides were stained with hematoxylin and eosin (H&E) for the characterization of morphology, malignancy, degree of differentiation and presence of necrosis. Microscopic observation was performed on a Nikon Eclipse 50i microscope equipped with digital camera Nikon Digital Sight DS-Fil.

Statistical Analysis

Statistical analysis was performed using IBM SPSS Statistics version 20, central tendency and dispersion measures were determined for descriptive analysis. For inferential analysis, normal distribution of quantitative variables was evaluated according to the Shapiro-Wilk's test.

Comparison of sphere-forming capacity, self-renewal, clonogenic efficiency, CD133, CD24 and CD44 expression was performed by one-way ANOVA when normal distribution and homogeneity of variances were present and by Kruskal-Wallis otherwise. Results obtained by western blot, including analysis of ALDH, ER α , ER β , PR, HER2, p53 and β -catenin expression, were compared using one sample Student's *t* test, comparing to the value 1. ¹⁸F-FDG uptake experimental values obtained for each condition were fitted to an exponential model using OriginPro software (OriginLab Corporation, Northampton, USA), version 8.0, according to Equation $\text{Uptake (\%)} = A \cdot (1 - e^{-\ln(2) \cdot t / T_{50\%}})$, *A*, maximum uptake, *T*_{50%}, time to half of the maximum uptake. These parameters were compared using the one-way ANOVA. For NMR studies, experimental concentration values of [U-¹³C]lactate for each time-point were fitted by linear regression for each cell population. Comparison of slopes was performed using one-way ANOVA. Comparison of C3_Lactate/C3_Alanine, C3_Lactate/C4_Glutamate, C4Q/C4D45 and C3_Glutamate/C4_Glutamate ratios between cell populations was performed using one-way ANOVA or Kruskal-Wallis, according to the previous conditions. In *in vivo* studies, comparison of time until tumour volume of 100 mm³ was obtained and the tumour volume at the end of 10 days was performed using one-way ANOVA or Kruskal-Wallis. When appropriate, multiple comparisons were performed using Bonferroni correction. A significance level of 5% was considered for all comparisons.

Results

The sphere-forming protocol originated spherical colonies of cells in suspension from ECC-1, G1, G2 and G3. The spheres ES1, ES2 and ES3 had spherical morphology, sometimes irregular, with surface projections of cells with variable sizes, shown in Fig. 1a). Derived adherent G1, G2 and G3 cells arose as proliferating cells that migrated from the periphery of the spheres and originated a confluent layer.

Sphere-Forming Capacity, Self-Renewal Capacity, Cloning Efficiency

The spheres-forming capacity for the ECC-1 cell line to originate ES1 was $2.22 \pm 0.93\%$, for G1 to originate ES2 was 2.54

$\pm 1.05\%$ and for G2 to originate ES3 was $2.40 \pm 0.85\%$, as shown in Fig. 1b). The self-renewal of spheres revealed $1.55 \pm 0.63\%$ for ES1 dissociation, $1.78 \pm 1.06\%$ for ES2 and $3.14 \pm 1.61\%$ for ES3, the latter being significantly higher than the former ($p = 0.002$), as shown in Fig. 1c). Spheres had a cloning efficiency lower than the ECC-1 cell line, $90.77 \pm 14.26\%$, of $23.71 \pm 8.49\%$ ($p < 0.001$) for ES1, of $14.62 \pm 6.66\%$ ($p < 0.001$) for ES2 and of $14.42 \pm 9.20\%$ ($p < 0.001$) for ES3. The derived adherent G1, G2 and G3 had a cloning efficiency not significantly different from the ECC-1 cell line, as shown in Fig. 1d).

CSC Markers

The mean fluorescence intensity (MFI) of CD133, shown in Fig. 2a), revealed that expression in ES3 was significantly higher than in ECC-1 ($p = 0.048$). The MFI of CD44, shown in Fig. 2b), evidenced no alterations in the expression considering the populations studied. The MFI for CD24, shown in Fig. 2c), highlighted that expression in ES1 was significantly higher than in ECC-1 ($p = 0.006$). Regarding ALDH expression, shown in Fig. 2d), it was significantly augmented in ES1 (1.41 ± 0.25 , $p = 0.014$), ES2 (1.86 ± 0.46 , $p = 0.001$) and ES3 (2.10 ± 0.46 , $p = 0.004$) compared to ECC-1. The ALDH expression in G1 (1.27 ± 0.26), G2 (1.36 ± 0.23) and G3 (1.27 ± 0.35) was not significantly different from ECC-1.

Molecular Markers

P53 expression, shown in Fig. 3a), was significantly lower in ES1 (0.46 ± 0.15 , $p = 0.006$), ES2 (0.61 ± 0.19 , $p = 0.06$) and ES3 (0.55 ± 0.16 , $p < 0.001$) compared to ECC-1. The P53 expression in G1 (0.97 ± 0.17), G2 (0.98 ± 0.15) and G3 (0.95 ± 0.19) was similar to ECC-1. β -catenin expression is shown in Fig. 3b) and was evaluated in ES1 (1.27 ± 0.10), ES2 (1.25 ± 0.24), ES3 (1.20 ± 0.05), G1 (0.71 ± 0.07), G2 (0.69 ± 0.12) and G3 (0.75 ± 0.06). For HER2 expression, represented in Fig. 3c), it was not possible to identify any marking band with the specific antibody used, therefore a whole protein extract from MCF-7 cell line was used as positive control. ER α expression, shown in Fig. 3d), was significantly lower in ES1 (0.060 ± 0.20 , $p < 0.001$), ES2 (0.36 ± 0.13 , $p < 0.001$) and ES3 (0.63 ± 0.24 , $p = 0.042$) compared to ECC-1. However, no differences were found for G1 (0.94 ± 0.08), G2 (1.06 ± 0.25) and G3 (0.88 ± 0.21). ER β expression, shown in Fig. 3e), in ES1 (0.97 ± 0.20), ES2 (1.15 ± 0.42), ES3 (1.05 ± 0.41), G1 (1.11 ± 0.47), G2 (1.08 ± 0.31) and G3 (1.02 ± 0.25) remained similar to ECC-1. Likewise, PR expression, shown in Fig. 3f), in ES1 (0.94 ± 0.15), ES2 (1.23 ± 0.10), ES3 (1.06 ± 0.21), G1 (1.06 ± 0.17), G2 (0.91 ± 0.11) and G3 (1.12 ± 0.13) was not significantly different from ECC-1.

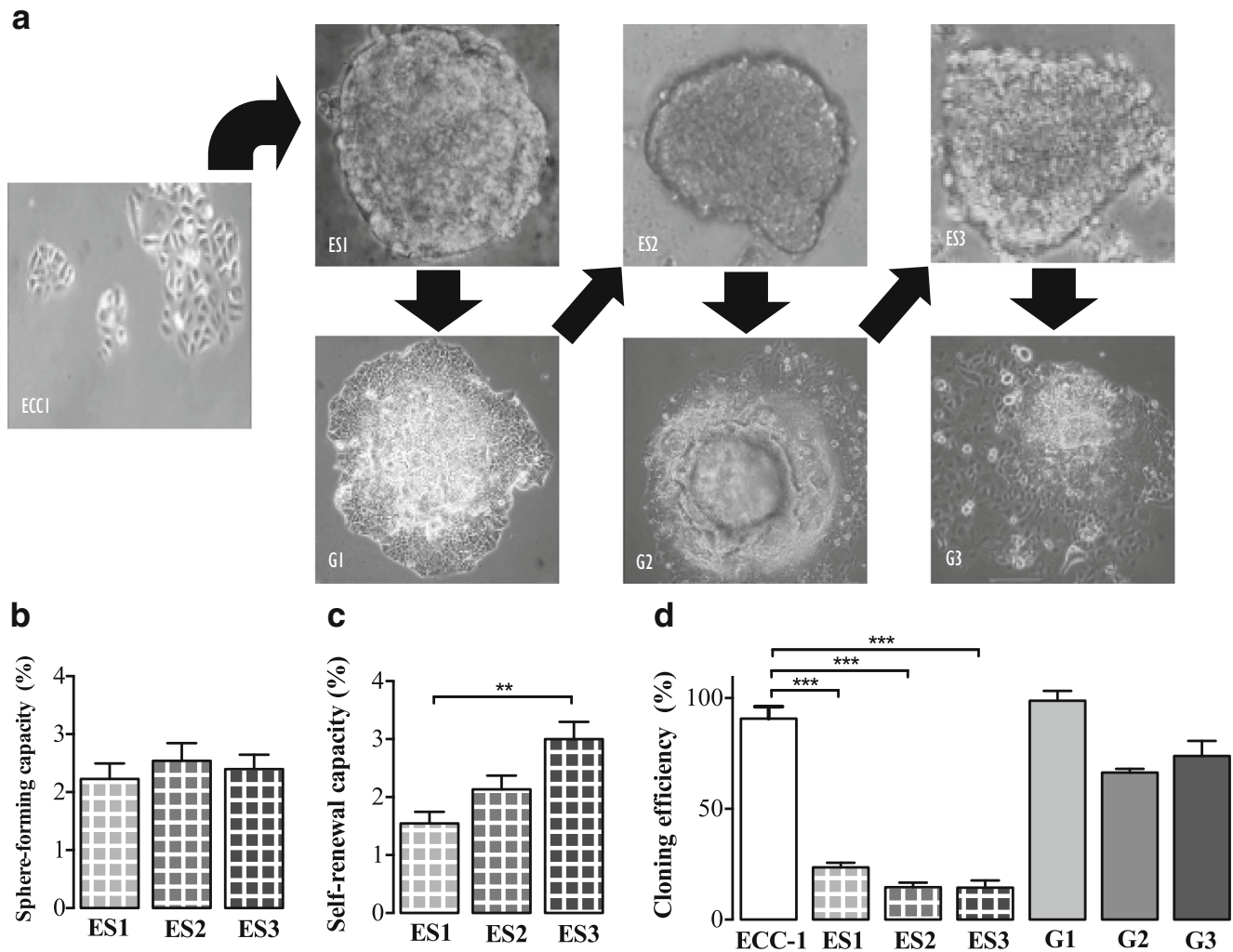


Fig. 1 **a** ECC-1 cell line, sphere populations (ES1, ES2 and ES3) and derived adherent populations (G1, G2 and G3). The arrows represent the succession of obtaining cell cultures. Images were obtained with a magnification of 400x. **b** Sphere-forming capacity of ES1, ES2 and ES3 expressed as the ratio between the number of spheres and the number of cells distributed. Results represent the mean and standard error of six experiments; there were no significant differences among populations. **c** Self-renewal of ES1, ES2 and ES3 expressed as percentage of the ratio

between the number of spheres obtained and the number of cells distributed. Results represent the mean and standard error of six experiments. **d** Cloning efficiency of ECC-1, ES1, ES2, ES3, G1, G2 and G3 expressed as the ratio between the number of colonies and the number of cells distributed. Results represent the mean and standard error of at least six experiments. The significant differences were represented with ** for $p < 0.01$ and *** for $p < 0.001$

Glucose Metabolism

The maximum ^{18}F -FDG uptake, Fig. 4a), was higher in spheres than in the parental cell line ECC-1 ($0.55 \pm 0.05\%$), with a value of $1.00 \pm 0.05\%$ ($p = 0.0076$) for ES1, $0.98 \pm 0.06\%$ ($p = 0.0062$) for ES2 and $1.04 \pm 0.09\%$ ($p = 0.018$) for ES3. There were no differences comparing ECC-1 and adherent population, with maximum uptake of $0.54 \pm 0.01\%$ in G1, $0.55 \pm 0.03\%$ in G2 and $0.66 \pm 0.07\%$ in G3.

The $[\text{U-}^{13}\text{C}]$ lactate production, whose expansion spectra is represented in Fig. 4b), increased with incubation time. The lactate production rate, Fig. 4c), decreased in ES1 in comparison with ECC-1 ($p < 0.001$)

and G1 ($p < 0.001$). The decrease in lactate output to the culture medium was indicative of a lower glycolytic activity in ES1. The ^{13}C -NMR spectra, showed that the $\text{C}_3\text{Lactate}/\text{C}_3\text{Alanine}$ ratio, represented in Fig. 4d), in ES1 (3.13 ± 1.61) was inferior to G1 (12.08 ± 6.52 , $p = 0.022$) and to ECC-1 (10.48 ± 2.32), pointing to an increased cytosolic oxidized state in ES1. The $\text{C}_3\text{Lactate}/\text{C}_4\text{Glutamate}$ ratio, shown in Fig. 4e), was lower in ES1 (7.52 ± 2.69) than ECC-1 (15.73 ± 1.27 , $p = 0.038$) and G1 (16.34 ± 4.79), indicating a higher coupling between glycolysis and Krebs cycle in ES1. The Krebs cycle turnover, evaluated by the $\text{C}_4\text{Q}/\text{C}_4\text{D}_4\text{S}$ ratio, presented in Fig. 4f), remained similar comparing ECC-1, ES1 and G1. Similarly, in the

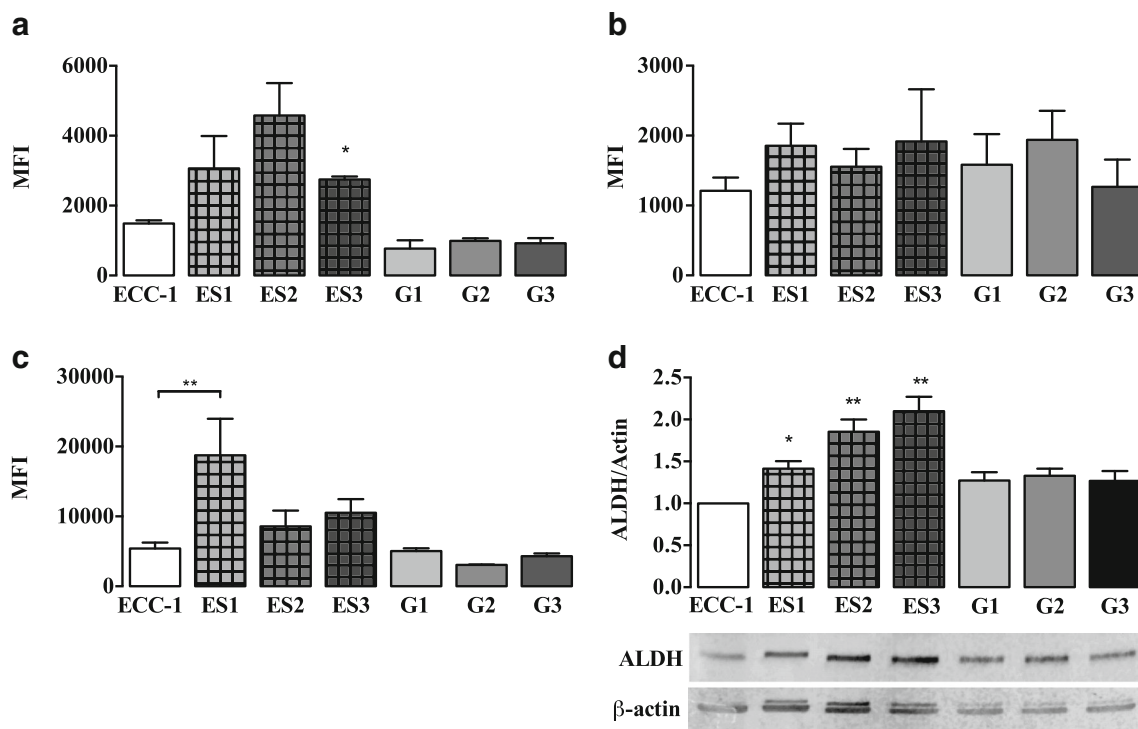


Fig. 2 **a** CD133, **b** CD24 and **c** CD44 expression using flow cytometry in ECC-1, ES1, ES2, ES3, G1, G2 and G3. The graphs express the MFI and standard error of at least three experiments. **d** ALDH expression in ECC-1, ES1, ES2, ES3, G1, G2 and G3. The results are presented as the ratio of the fluorescence intensities of ALDH and β -actin and the graphs

represent the variation in relation to the expression of ECC-1 cell line (ALDH/ β -actin equal to 1). The values presented express the mean and standard error of at least four experiments. The images represent an immunoblot of ALDH and β -actin expression for each experimental condition. The significant differences were represented with * for $p < 0.05$ and ** for $p < 0.01$

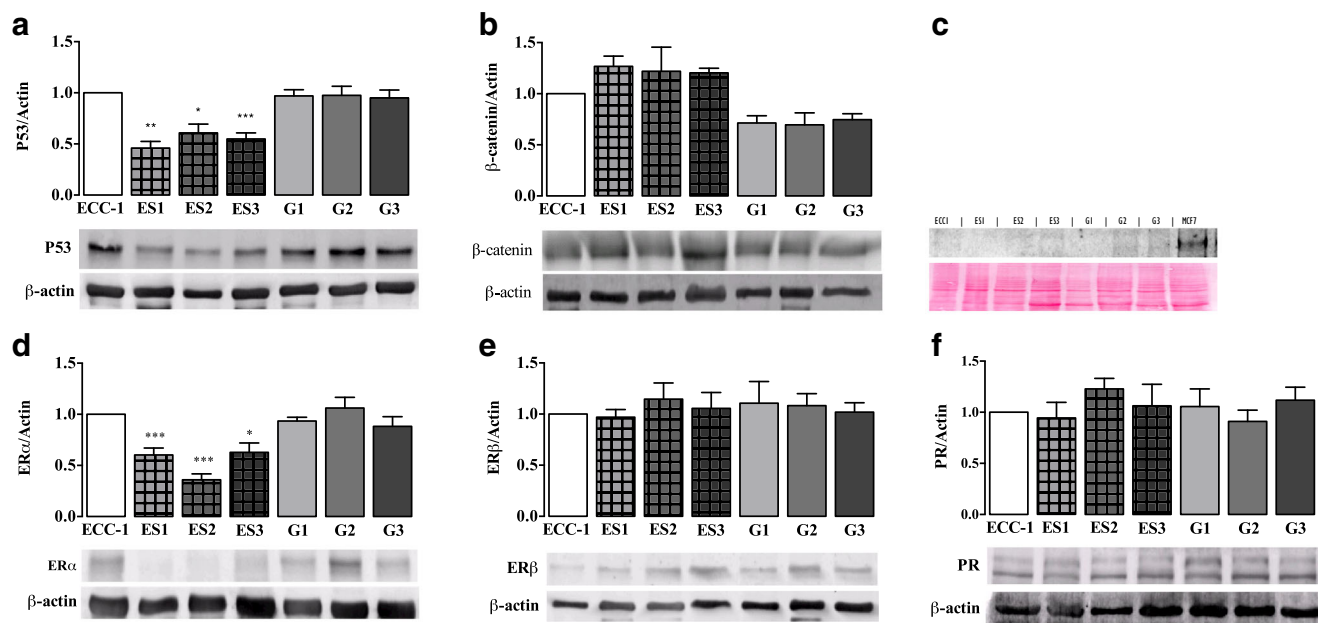


Fig. 3 **a** P53, **b** β -catenin, **c** HER2, **d** ER α , **e** ER β and **f** PR expression in ECC-1, ES1, ES2, ES3, G1, G2 and G3. The results are presented as the ratio of the fluorescence intensities of P53, β -catenin, ER α , ER β and PR versus actin and the graphs represent the alteration in relation to the ECC-1 cell line (protein of interest/ β -actin equal to 1). The values presented express the mean and standard error of at least four experiments. Significant differences from ECC-1 cell line were represented with *

$p < 0.05$, ** $p < 0.01$ and *** $p < 0.001$. The images represent an immunoblot of P53, β -catenin, ER α , ER β and PR and actin expression for each experimental condition. **c** Representative immunoblot of HER2 expression in the ECC-1 cell line, ES1, ES2, ES3, G1, G2 and G3. The MCF-7 cell line was used as positive control. Below is represented an image of the same membrane previously submitted staining with Ponceau

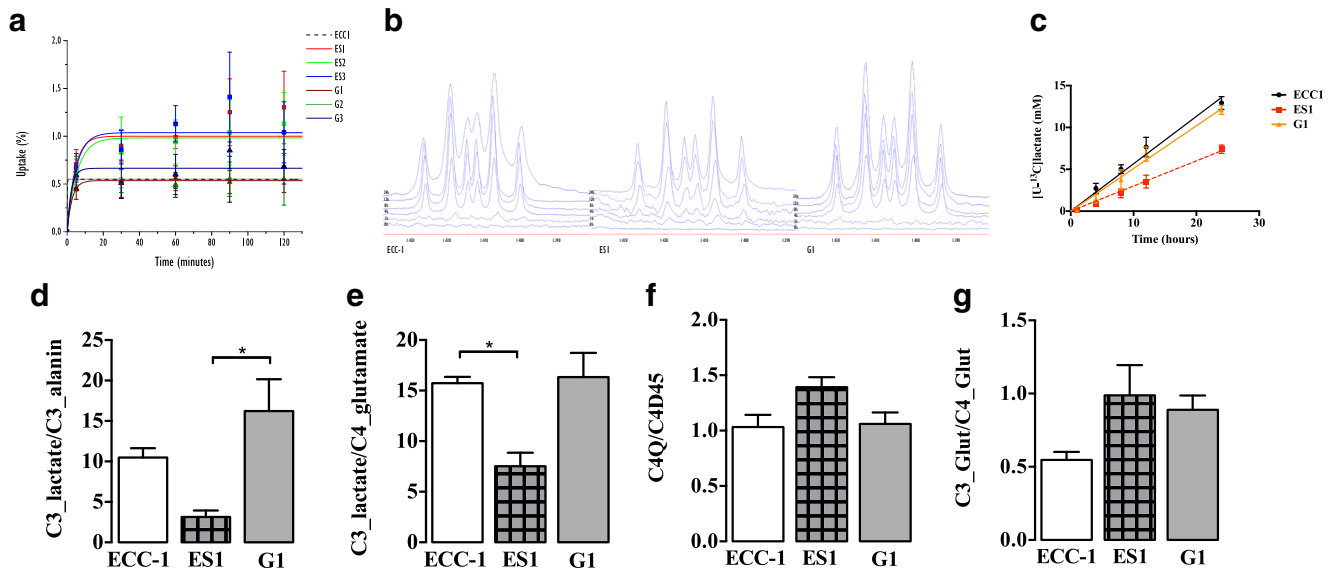


Fig. 4 **a** ^{18}F -FDG uptake in ECC-1, ES1, ES2, ES3, G1, G2 and G3. The values express the mean and standard error of the uptake percentage at 5, 30, 60, at 90 and 120 min of at least 4 experiments, $R^2 > 0.95$ for all groups. **b** Expansions of ^1H -NMR spectra of the culture medium of ECC-1 cells, ES1 and G1 relating to one of the satellites of $[\text{U-}^{13}\text{C}]$ lactate. Resonance is composed of six peaks, resulting from the existence of homo couplings ($^3J_{\text{HH}}$) and heteronuclear ($^2J_{\text{HC}}$ e $^3J_{\text{HC}}$). Samples were referring to 0, 1, 4, 8, 12 and 24 h. **c** Concentration of $[\text{U-}^{13}\text{C}]$ lactate in the culture medium during 24 h incubation for ECC-1, ES1 and G1

populations. The values presented express the average and standard error of at least four experiments, for each time. The slope (mM/h) for ECC-1 it was 0.57 ± 0.02 ($r^2 = 0.93$), for ES1 was 0.30 ± 0.01 ($r^2 = 0.91$) and for G1 was 0.51 ± 0.02 ($r^2 = 0.92$). **d** C3_lactate/C3_alanine ratio, **e** C3_Lactate/C4_glutamate ratio, **f** C4Q/C4D45 ratio and **g** C3_glutamate/C4_glutamate ratio for ECC-1, ES1 and G1. The values presented express the mean and standard error of at least four experiments. Significant differences from ECC-1 cell line were represented with * $p < 0.05$

C3_Glutamate/C4_Glutamate ratio, shown in Fig. 4g), no significant differences were found between the populations.

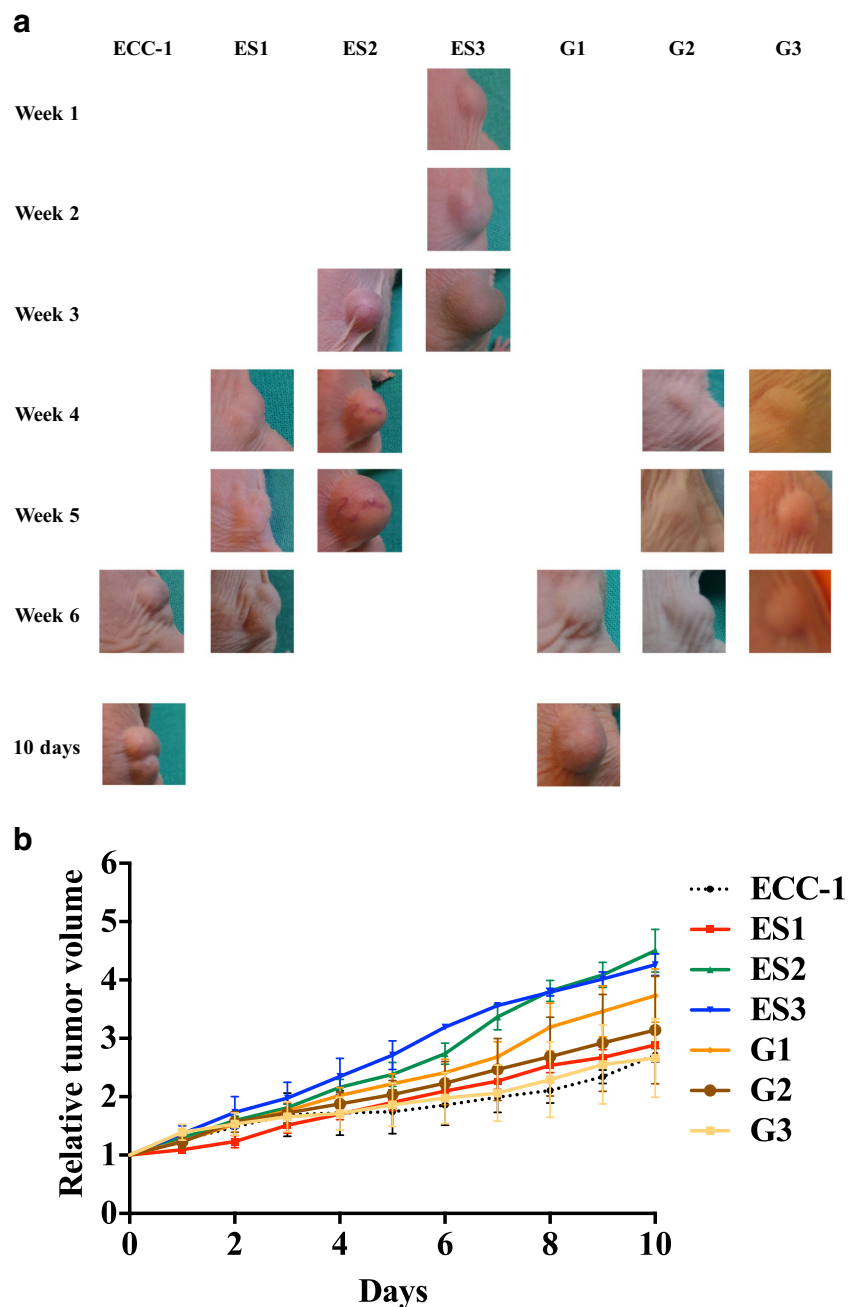
The Fig. 5a) represents an example of animals from each group monitored weekly after obtaining a tumour volume of 100 mm^3 . The evaluation of tumour growth points to an earlier onset of tumours in ES3 xenotransplantation, identified in the first week. The resulting tumours from ECC-1 (37.8 ± 9.9 days) and G1 (40.0 ± 1.4 days) were those which took longer to reach a volume of 100 mm^3 . On the contrary, ES3 cells originated this volume in only 3.7 ± 1.2 days.

The same outcome for ES1 was 27.5 ± 15.2 days, for ES2 it was at 23.8 ± 9.0 days, for G2 it was at 24.5 ± 4.5 days and for G3 4.7 ± 2.1 days, thus not showing any statistically significant differences. Considering the relative tumour volume in the 10 days after reaching 100 mm^3 , shown in Fig. 5b), the growth was superior for ES2 (4.50 ± 0.64) and ES3 (4.26 ± 0.32); however, the growth pattern was not significantly different from ECC-1 (2.71 ± 0.20), ES1 (2.89 ± 0.45), G1 (3.73 ± 0.79), G2 (3.14 ± 1.30) and G3 (2.66 ± 1.16). The histological study, represented in Fig. 6 revealed that the xenografts correspond to malignant epithelial tumors with similar characteristics to each other, consisting mainly of solid areas with glandular tissue in a minor proportion. The cells are polygonal, with eosinophilic cytoplasm and pleomorphic hyperchromatic nuclei. There are mitoses, atypia and necrotic areas.

Discussion

This experimental study evaluated the spheres of endometrial cancer cells and the derived adherent cells which had the capacity to differentiate in the original phenotype. Studies based on sphere protocol have been largely used to evaluate the activity of normal and tumour stem cells [1, 23]. This population was described for various solid tumours, particularly for breast cancer, prostate cancer, colorectal cancer, gliomas, pancreatic cancer, hepatocellular carcinoma and lung cancer [1]. The model of tumorspheres allows the study of CSC and has been applied in various fields such as the evaluation of tumour growth, stemness, tumorigenicity in vivo and sensitivity to drugs. The supplementation with bFGF and EGF ensures the maintenance of spheres and other stem cells, including embryonic stem cells, are not fully understood. Regarding bFGF, it regulates the level and post-transcriptional state of several target molecules affecting cell self-renewal, cell survival, cell proliferation, cell adhesion and suppression of terminal differentiation [24]. In the sphere-forming protocol, each sphere is derived from the clonal growth of a single cell being distributed at low density in semisolid media to prevent cell fusion and aggregation [15]. This inhibition of cell adhesion causes the death of differentiated cells by anoikis [25]. The sphere-forming protocol was repeated successively from cultures of adherent populations derived from spheres. The successive sphere-forming protocol reflects the self-renewal capacity.

Fig. 5 a Illustrative photographic record of tumour growth after obtaining a volume of 100 mm^3 . **b** Tumour growth of ECC-1, ES1, ES2, ES3, G1, G2 and G3. The values presented express the mean and standard error of at least three experiments; the results express the relative tumour volume (tumour volume/ 100 mm^3)



Other authors observed self-renewal and differentiation of spheres, addressing its plasticity [26].

The sphere-forming capacity previously showed an apparently specific variability of each line [27]. The self-renewal capacity indicates that the sphere population is heterogeneous, with a small proportion of cells with symmetric division capacity. In our study, the increase in self-renewal capacity between ES1 and ES3 may be indicative of a subsequent enrichment of stemness properties. The clonogenic efficiency obtained in our experimental study showed a lower ability to form colonies in spheres compared with the ECC-1 cell line and adherent populations. Thus, this suggests the need for a

period of adaptation prior to switching to adherent conditions, while confirming the plasticity of the spheres population [28].

In our study, CD133 expression was higher in spheres ES1, ES2 and ES3, particularly regarding the latter, which may also be indicative of enhanced stemness. Studies with tumorspheres from other tumours reported a higher percentage of CD133⁺ superior than monolayer culture [29, 30]. Our study showed a higher expression of CD44 in spheres, significant in ES1 and values of adherent populations, consistent with the loss of CD44 expression with differentiation. Previous studies on CSC showed high levels of ALDH suggesting that ALDH activity may be a common marker for the

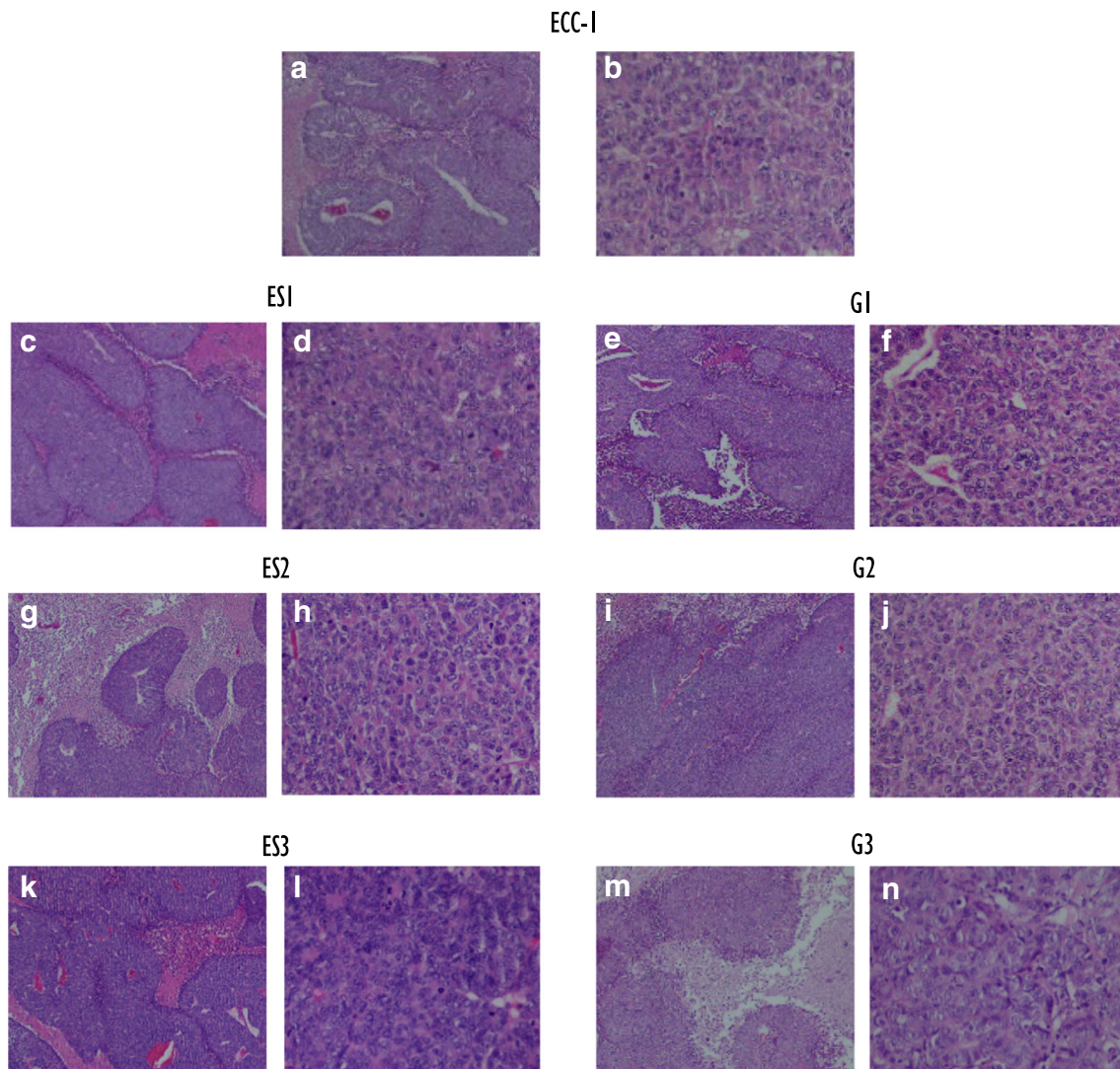


Fig. 6 Histological images representative of heterotopic tumours stained with hematoxylin and eosin from animals injected with ECC-1 (**a** and **b**), ES1 (**c** and **d**), G1 (**e** and **f**) ES2 (**g** and **h**), G2 (**i** and **j**), ES3 (**k** and **l**), G3 (**m** and **n**). Histological images represent predominantly

solid tumours with a minor glandular component. The cells have high cytonuclear atypia, high mitotic index and some areas of necrosis. For each pair of images, the left has a magnification of 40x and the right of 200x

stem cell population in normal and malignant tissue [31]. ALDH expression was associated with spheres of other types of cancer, including ovary, colorectal and neuroblastoma [30, 32]. These studies also showed decreased ALDH expression with differentiation into adherent conditions.

In breast and lung tumours, P53 reduced CD44 expression by inhibiting transcription, which resulted in decreased tumorigenicity [33]. In our study the decrease of P53 in spheres was accompanied by an increase in CD44 expression which correlates with the loss of P53 repression. β -catenin expression in spheres showed an increasing trend compared to ECC-1. Other studies with CSC had increased β -catenin activity [29, 34]. The WNT/ β -catenin pathway regulates endometrial proliferation and differentiation and is activated in endometrial

carcinoma [35]. In association, the decrease in ER α expression in endometrial spheres, observed in our study, may have implications for activation not only of the WNT pathway but also of the PI3K/AKT/mTOR pathway also involved in cell proliferation and survival.

In the initial stage of endometrial repair the epithelial cells do not express ER α which are only expressed during proliferation and differentiation phase of epithelial glandular cells and to a lesser extent, in stromal cells [36]. The loss of ER α was accompanied by an increase in ALDH, and was corroborated by other authors who reported endometrium tumour cells with ALDH expression being ER negative [13]. Thus, the loss of these receptors might reveal a more undifferentiated phenotype and relate to EMT in hormone-dependent tumours. Spheres, where decreased

α isoform was observed, maintain the β isoform expression which may be responsible for a proliferation-promoting effect on these cells [37].

The spheres' increased ^{18}F -FDG uptake may be explained by the lower expression of P53 since the uptake of this radiopharmaceutical is dependent on its function [38]. The Warburg effect, which defines the dependence of cancer on fermentative glycolysis, is required for tumour cells to resist oxidative stress and be able to adapt to hypoxia conditions. This metabolic shift may be an early or late event or be a genetically determined dysfunction or induced by metabolic changes [39]. The intracellular fate of glucose was evaluated in further detail by monitoring the incorporation of ^{13}C into metabolic intermediates resulting from $[\text{U-}^{13}\text{C}]$ glucose metabolism in ECC-1, ES1 and G1. The $[\text{U-}^{13}\text{C}]$ lactate production was lower over 24 h in ES1 compared to ECC-1 and G1, which indicates the preferential use of fermentative glycolysis by ECC-1 and G1. Moreover, the redox state in the cytosol, inferred by the relationship C3_Lac/C3_Ala , was lower in ES1 compared to ECC-1. The coupling of the glycolytic pathway to the Krebs cycle was increased in ES1 compared to ECC-1 and G1, allowing a more complete oxidation of glycolytic intermediates. There are some studies that associate the metabolism of CSC to fermentative glycolysis instead of mitochondrial oxidative phosphorylation [40]. However, other studies have indicated a metabolic state associated with oxidative phosphorylation, unlike the Warburg effect [41]. Our results suggest that in CSC of endometrial origin oxidative phosphorylation assumes more relevance and that a higher avidity for glucose is also present, compared to the parental cell line.

The relative tumour volume was higher in ES3 and ES2, which points to a greater capacity for initiation and maintenance of tumour growth. In another study of endometrial cancer, tumorspheres also had larger tumours than differentiated cells [10]. Also, the CD133^+ population from a human endometrial tumours was more tumorigenic than the main population [12]. These data are consistent with the presence of a population of CSC with tumorigenic capacity *in vivo*.

Tumorspheres are not a homogeneous structure of undifferentiated cells but include a variability of morphologically distinct entities with molecular heterogeneity inter- and intrasphere. The sphere protocol selectively enriches the CSC growth, albeit also progenitor cells and differentiated tumour cells [25]. In fact, the aim of successively repeating the protocol was to isolate a group of cells with the highest prevalence of stem properties, as well as checking the maintenance of self-renewal properties. The enhanced stemness of ES3 was emphasized by higher self-renewal, CD133 and ALDH expression and tumorigenicity *in vivo* than the first sphere generation. Globally, these and the other findings

of this work, namely, stem cell markers and molecular markers of differentiation, suggest an analogous profile and highlight spheres with CSC properties compared to adherent populations.

This experimental work used a successive sphere protocol in endometrial cancer that isolated a late generation (ES3) with higher stemness properties considering self-renewal capacity, CD133 expression and tumorigenicity. Generally, the spheres had higher expression of CSC markers, namely CD133, CD44 and ALDH and tumorigenicity *in vivo* than adherent populations. A more undifferentiated phenotype, revealed by a decrease in $\text{ER}\alpha$, the decrease in P53 expression and the activation of β -catenin pathway, were associated with the spheres' phenotype. Furthermore, the glucose metabolism in spheres revealed an increased uptake associated with complete oxidation instead of the Warburg effect, which is more globally associated with cancer populations. The strategy used to isolate CSC pointed to a population with a molecular and metabolic profile suitable to be used in the future as a model for other studies such as research of tumour markers and targeted therapies.

Acknowledgements This study was funded by the Foundation for Science and Technology, Portugal, through individual support to Carvalho MJ (SFRH/SINTD/60068/2009), by the Portuguese Society of Gynecology through the 2016 Research Prize and by CIMAGO. CNC.IBILI is supported through the Foundation for Science and Technology, Portugal (UID/NEU/04539/2013), and co-funded by FEDER-COMPETE (POCI-01-0145-FEDER-007440).

The NMR spectrometer is part of the National NMR Network and was purchased as part of the Portuguese National Programme for Scientific Re-equipment (REDE/1517/RMN/2005), with funds from POCI 2010 (European Fund for Regional Development) and from the Foundation for Science and Technology, Portugal. The authors thank to the Pathology Service of the University Hospital Centre of Coimbra for technical support and David Anthony Tucker for the manuscript review.

Compliance with Ethical Standards

Conflicts of Interest Nothing to declare.

Ethics Approval The experimental protocol was approved by the Ethics Committee of the Medicine Faculty of Coimbra University (Ref: Of IBB/48/09). All experiments were performed in accordance with guidelines and regulations of the European Union.

Abbreviations *ALDH*, aldehyde dehydrogenase; *ATCC*, American Type Culture Collection; *bFGF*, basic fibroblast growth factor; *BSA*, bovine serum albumin solution; *CPM*, counts per minute; *CSC*, cancer stem cells; *ECC-1*, human endometrioid carcinoma type I cell line; *EGF*, epidermal growth factor; *EMT*, epithelial to mesenchymal transition; *ER*, oestrogen receptors; *ES1*, first sphere generation; *ES2*, second sphere generation; *ES3*, third sphere generation; *^{18}F -FDG*, fluorine-18 fluorodeoxyglucose; *G1*, first generation of adherent cells derived from the spheres; *G2*, second generation of adherent cells derived from the spheres; *G3*, third generation of adherent cells derived from the spheres; H&E, hematoxylin and eosin; *MFI*, mean fluorescence intensity; *PR*, progesterone

receptors; *RPMI*, Rooswell Park Memorial Institute 1640 Medium; *TBS-T*, Tris-buffered saline Tween-20; [*U-13C*], uniformly enriched ¹³C isotopomer glucose

References

- Allegra A, Alonci A, Penna G, Innao V, Gerace D, Rotondo F, Musolino C (2014) The cancer stem cell hypothesis: a guide to potential molecular targets. *Cancer Investig* 32:470–495. <https://doi.org/10.3109/07357907.2014.958231>
- Chan RWS, Schwab KE, Gargett CE (2004) Clonogenicity of human endometrial epithelial and stromal cells. *Biol Reprod* 70:1738–1750. <https://doi.org/10.1095/biolreprod.103.024109>
- Kato K, Yoshimoto M, Kato K, Adachi S, Yamayoshi A, Arima T, Asanoma K, Kyo S, Nakahata T, Wake N (2007) Characterization of side-population cells in human normal endometrium. *Hum Reprod* 22:1214–1223. <https://doi.org/10.1093/humrep/del514>
- Chan RWS, Gargett CE (2006) Identification of label-retaining cells in mouse endometrium. *Stem Cells (Dayton, Ohio)* 24:1529–1538. <https://doi.org/10.1634/stemcells.2005-0411>
- Carvalho MJ, Laranjo M, Abrantes AM, Torgal I, Botelho MF, Oliveira CF (2015) Clinical translation for endometrial cancer stem cells hypothesis. *Cancer Metastasis Rev* 34:401–416. <https://doi.org/10.1007/s10555-015-9574-0>
- Hubbard SA, Friel AM, Kumar B et al (2009) Evidence for cancer stem cells in human endometrial carcinoma. *Cancer Res* 69:8241–8248. <https://doi.org/10.1158/0008-5472.CAN-08-4808>
- Kato K, Takao T, Kuboyama A, Tanaka Y, Ohgami T, Yamaguchi S, Adachi S, Yoneda T, Ueoka Y, Kato K, Hayashi S, Asanoma K, Wake N (2010) Endometrial cancer side-population cells show prominent migration and have a potential to differentiate into the mesenchymal cell lineage. *Am J Pathol* 176:381–392. <https://doi.org/10.2353/ajpath.2010.090056>
- Kusunoki S, Kato K, Tabu K, Inagaki T, Okabe H, Kaneda H, Suga S, Terao Y, Taga T, Takeda S (2013) The inhibitory effect of salinomycin on the proliferation, migration and invasion of human endometrial cancer stem-like cells. *Gynecol Oncol* 129:598–605. <https://doi.org/10.1016/j.ygyno.2013.03.005>
- Götte M, Greve B, Kelsch R et al (2011) The adult stem cell marker *Musashi-1* modulates endometrial carcinoma cell cycle progression and apoptosis via Notch-1 and p21 WAF1/CIP1. *Int J Cancer* 129:2042–2049. <https://doi.org/10.1002/ijc.25856>
- Zhou X, Zhou Y-P, Huang G-R et al (2011) Expression of the stem cell marker, *Nanog*, in human endometrial adenocarcinoma. *Int J Gynecol Pathol* 33:262–270. <https://doi.org/10.1097/PGP.0b013e3182055a1f>
- Rutella S, Bonanno G, Procoli A et al (2009) Cells with characteristics of cancer stem/progenitor cells express the CD133 antigen in human endometrial tumors. *Clin Cancer Res* 15:4299–4311. <https://doi.org/10.1158/1078-0432.CCR-08-1883>
- Friel AM, Zhang L, Curley MD et al (2010) Epigenetic regulation of CD133 and tumorigenicity of CD133 positive and negative endometrial cancer cells. *Reprod Biol Endocrinol* 8:147. <https://doi.org/10.1186/1477-7827-8-147>
- Rahadiani N, Ikeda J, Mamat S, Matsuzaki S, Ueda Y, Umehara R, Tian T, Wang Y, Enomoto T, Kimura T, Aozasa K, Morii E (2011) Expression of aldehyde dehydrogenase 1 (ALDH1) in endometrioid adenocarcinoma and its clinical implications. *Cancer Sci* 102:903–908. <https://doi.org/10.1111/j.1349-7006.2011.01864.x>
- Tang DG (2012) Understanding cancer stem cell heterogeneity and plasticity. *Cell Res* 22:457–472. <https://doi.org/10.1038/cr.2012.13>
- Dontu G, Abdallah WM, Foley JM, Jackson KW, Clarke MF, Kawamura MJ, Wicha MS (2003) In vitro propagation and transcriptional profiling of human mammary stem/progenitor cells. *Genes Dev* 17:1253–1270. <https://doi.org/10.1101/gad.1061803>
- Ponti D, Costa A, Zaffaroni N, Pratesi G, Petrangolini G, Coradini D, Pilotti S, Pierotti MA, Daidone MG (2005) Isolation and in vitro propagation of tumorigenic breast cancer cells with stem/progenitor cell properties. *Cancer Res* 65:5506–5511. <https://doi.org/10.1158/0008-5472.CAN-05-0626>
- Wilson H, Huelsmeyer M, Chun R, Young KM, Friedrichs K, Argyle DJ (2008) Isolation and characterisation of cancer stem cells from canine osteosarcoma. *Vet J* 175:69–75. <https://doi.org/10.1016/j.tvjl.2007.07.025>
- Franken N a P, Rodermond HM, Stap J et al (2006) Clonogenic assay of cells in vitro. *Nat Protoc* 1:2315–2319. <https://doi.org/10.1038/nprot.2006.339>
- Santos K, Laranjo M, Abrantes AM, Brito AF, Gonçalves C, Sarmento Ribeiro AB, Botelho MF, Soares MIL, Oliveira ASR, Pinho e Melo TMVD (2014) Targeting triple-negative breast cancer cells with 6,7-bis(hydroxymethyl)-1H,3H-pyrrolo[1,2-c]thiazoles. *Eur J Med Chem* 79:273–281. <https://doi.org/10.1016/j.ejmech.2014.04.008>
- Abrantes AM, Serra MES, Gonçalves AC, Rio J, Oliveiros B, Laranjo M, Rocha-Gonsalves AM, Sarmento-Ribeiro AB, Botelho MF (2010) Hypoxia-induced redox alterations and their correlation with 99mTc-MIBI and 99mTc-HL-91 uptake in colon cancer cells. *Nucl Med Biol* 37:125–132. <https://doi.org/10.1016/j.nucmedbio.2009.11.001>
- Carvalho RA, Rodrigues TB, Zhao P et al (2004) A ¹³C isotopomer kinetic analysis of cardiac metabolism: influence of altered cytosolic redox and [Ca²⁺]_o. *Am J Phys Heart Circ Phys* 287:H889–H895. <https://doi.org/10.1152/ajpheart.00976.2003>
- Sherry AD, Jeffrey FMH, Malloy CR (2004) Analytical solutions for ¹³C isotopomer analysis of complex metabolic conditions: substrate oxidation, multiple pyruvate cycles, and gluconeogenesis. *Metab Eng* 6:12–24. <https://doi.org/10.1016/j.ymben.2003.10.007>
- Visvader JE, Lindeman GJ (2008) Cancer stem cells in solid tumours: accumulating evidence and unresolved questions. *Nat Rev Cancer* 8:755–768. <https://doi.org/10.1038/nrc2499>
- Nieto-Estévez V, Pignatelli J, Araúzo-Bravo MJ, Hurtado-Chong A, Vicario-Abejón C (2013) A global transcriptome analysis reveals molecular hallmarks of neural stem cell death, survival, and differentiation in response to partial FGF-2 and EGF deprivation. *PLoS One* 8:e53594. <https://doi.org/10.1371/journal.pone.0053594>
- Weiswald L-B, Bellet D, Dangles-Marie V (2015) Spherical Cancer models in tumor biology. *Neoplasia* 17:1–15. <https://doi.org/10.1016/j.neo.2014.12.004>
- Prasetyanti PR, Zimmerlin C, De Sousa E, Melo F, Medema JP (2013) Isolation and propagation of colon cancer stem cells. *Methods Mol Biol (Clifton, NJ)* 1035:247–259. https://doi.org/10.1007/978-1-62703-508-8_21
- Bortolomai I, Canevari S, Facetti I, de Cecco L, Castellano G, Zacchetti A, Alison MR, Miotti S (2010) Tumor initiating cells: development and critical characterization of a model derived from the A431 carcinoma cell line forming spheres in suspension. *Cell Cycle* 9:1194–1206. <https://doi.org/10.4161/cc.9.6.11108>
- Liu Y, Nenutil R, Appleyard MV, Murray K, Boylan M, Thompson AM, Coates PJ (2014) Lack of correlation of stem cell markers in breast cancer stem cells. *Br J Cancer* 110:2063–2071. <https://doi.org/10.1038/bjc.2014.105>
- Chung L, Tang S, Wu Y et al (2015) Galectin-3 augments tumor initiating property and tumorigenicity of lung cancer through interaction with β-catenin. *Oncotarget* 6:4936–4952. <https://doi.org/10.18632/oncotarget.3210>

30. Kryczek I, Liu S, Roh M, Vatan L, Szeliga W, Wei S, Banerjee M, Mao Y, Kotarski J, Wicha MS, Liu R, Zou W (2012) Expression of aldehyde dehydrogenase and CD133 defines ovarian cancer stem cells. *Int J Cancer* 130:29–39. <https://doi.org/10.1002/ijc.25967>
31. Tirino V, Desiderio V, Paino F, de Rosa A, Papaccio F, la Noce M, Laino L, de Francesco F, Papaccio G (2013) Cancer stem cells in solid tumors: an overview and new approaches for their isolation and characterization. *FASEB J* 27:13–24. <https://doi.org/10.1096/fj.12-218222>
32. Hartomo T, Van Huyen Pham T, Yamamoto N et al (2014) Involvement of aldehyde dehydrogenase 1A2 in the regulation of cancer stem cell properties in neuroblastoma. *Int J Oncol* 46:1089–1098. <https://doi.org/10.3892/ijo.2014.2801>
33. Rivlin N, Koifman G, Rotter V (2014) P53 orchestrates between Normal differentiation and Cancer. *Semin Cancer Biol* 32:10–17. <https://doi.org/10.1016/j.semcancer.2013.12.006>
34. Cui J, Li P, Liu X et al (2015) Abnormal expression of the notch and Wnt/ β -catenin signaling pathways in stem-like ALDHhiCD44+ cells correlates highly with Ki-67 expression in breast cancer. *Oncol Lett* 9:1600–1606. <https://doi.org/10.3892/ol.2015.2942>
35. Wang Y, van der Zee M, Fodde R, Blok LJ (2010) Wnt/B-catenin and sex hormone signaling in endometrial homeostasis and cancer. *Oncotarget* 1:674–684. <https://doi.org/10.18632/oncotarget.101007>
36. Gargett CE, Chan RWS, Schwab KE (2008) Hormone and growth factor signaling in endometrial renewal: role of stem/progenitor cells. *Mol Cell Endocrinol* 288:22–29. <https://doi.org/10.1016/j.mce.2008.02.026>
37. Hapangama DK, Kamal a M, Bulmer JN (2014) Estrogen receptor : the guardian of the endometrium. *Hum Reprod Update* 21:174–193. <https://doi.org/10.1093/humupd/dmu053>
38. R a G, Gillies RJ (2004) Why do cancers have high aerobic glycolysis? *Nat Rev Cancer* 4:891–899. <https://doi.org/10.1038/nrc1478>
39. Morfouace M, Lalier L, Bahut M, Bonnamain V, Naveilhan P, Guette C, Oliver L, Gueguen N, Reynier P, Vallette FM (2012) Comparison of spheroids formed by rat glioma stem cells and neural stem cells reveals differences in glucose metabolism and promising therapeutic applications. *J Biol Chem* 287:33664–33674. <https://doi.org/10.1074/jbc.M111.320028>
40. Palorini R, Votta G, Balestrieri C, Monestiroli A, Olivieri S, Vento R, Chiaradonna F (2014) Energy metabolism characterization of a novel cancer stem cell-like line 3AB-OS. *J Cell Biochem* 115:368–379. <https://doi.org/10.1002/jcb.24671>
41. Jang H, Yang J, Lee E, Cheong J-H (2015) Metabolism in embryonic and cancer stemness. *Arch Pharm Res* 38:381–388. <https://doi.org/10.1007/s12272-015-0558-y>